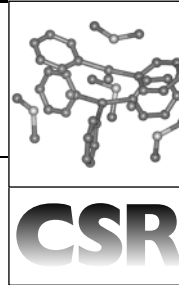# Decoding the 'black box' reactivity that is organocuprate conjugate addition chemistry

Simon Woodward

School of Chemistry, The University of Nottingham, University Park, Nottingham UK NG7 2RD.
*E-mail: simon.woodward@nottingham.ac.uk*

Understanding of the 1,4-addition of organocuprates, especially LiCuR$_2$ species, to enone Michael acceptors has blossomed in the light of recent kinetic, NMR, and theoretical investigations. These investigations have been reviewed and are compared to the various reaction co-ordinates they support. Emphasis is placed on relating the theoretical calculations to physical data extracted from real systems. The mechanism of cuprate conjugate addition is compared to related reactions including: additions to ynones, alkene carbocupration, and S_N2' allylic and propargylic substitution reactions.

1   Introduction

Organocuprates [**M**(Cu**R**$_2$)]$_n$ arguably constitute *the* superlative reagents for 1,4-addition (sometimes called *conjugate addition*) of '**MR**' to α,β-unsaturated systems (primarily enones), as shown in Scheme 1. This transformation has two attractive features: first, the product enolate may be trapped with a wide variety of electrophiles; secondly, for appropriately substituted enones a new stereogenic centre is generated. This high synthetic utility has caused cuprate methodology to be widely embraced over the past 30 years but has simultaneously resulted in a downplaying of the mechanisms by which these transformations occur. Recently, significant inroads into structure and behaviour of organocopper reagents have started to pull away the 'black box' veil from these remarkable reactions. While many excellent texts[1–2] and reviews[3–4] cover synthetic applications of organocuprate chemistry, it is the purpose of this article to survey literature relevant to the mechanism of 1,4-addition of cuprates to enones. Cuprate structure is covered
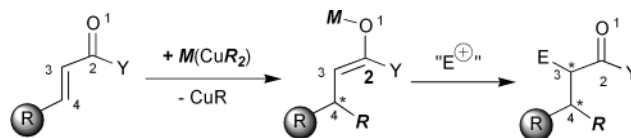
Scheme 1 Cuprate mediated 1,4-addition of '**MR**' to α,β-unsaturated systems (enones). R and Y represent generic groups. The 'E+' source may be H+, RI, RCHO, *etc.*

first, followed by studies relevant to the reaction co-ordinate in cuprate conjugate addition. Finally, comparisons with other reactions mechanistically related to these 1,4-additions are made. Throughout this review the numbering of Scheme 1 *viz.* O(1)–C(2)–C(3)–C(4) will be used for the enone connectivity.

2   Cuprate structure—it's an anion–cation world

2.1   The basics of cuprate structure

All cuprate reagents that take place in conjugate '**MR**' additions may be considered to be composed of [CuR$_n$]$^{m-}$ fragments, normally [CuR$_2$]$^-$, associated with counter cations M^{x+}. The apparent complexity of many organocuprate species can be rationalised by understanding the general behaviour of the constituent anions and cations alone and the general principles of how these fragments aggregate into what are effectively intimate contact ion pairs.

Cuprate reagents are normally formed by the reaction of main group organometallics (MR) with copper(I) salts (CuX), where X is a halide or pseudohalide. The natures of both M and X have profound effects on the structures and reactivities of the derived cuprates. Let us consider halides first. As halides co-ordinate Cu^I relatively weakly they are readily displaced from copper and a linear [R–Cu–R]$^-$ **1** unit is formed when *two* equivalents of MR are used [eqn (1), $n = 2$, in Scheme 2]. This linear Cu^I d^{10} arrangement **1** (Scheme 2) is the cornerstone building block of all cuprate structures. Structure **1** is frequently referred to as a *lower order cuprate*. Organolithiums (LiR) are often used to realise such transformations and cuprates having the stoichiometry LiCuR$_2$, containing fragment **1**, are additionally called *Gilman reagents* in honour of the reaction's originator.[5] Modification of the lithium to bulky cations allows these archetypal [CuR$_2$]$^-$ **1** units to be crystallographically characterised, as in Li(12-crown-4)$_2$[CuPh$_2$] (Fig. 1).[6] About half a dozen related structures are known and in these simple cases the C$_\alpha$–Cu–C$_\alpha$ unit is essentially linear (178.5–180.0°) with Cu–C$_\alpha$ distances ranging 1.915–1.935 Å. In contrast, if the precursor CuX contains a relatively strong Cu–X bond (for example, cyanide CN$^-$, thiolates RS$^-$, or phosphides R$_2$P$^-$) then the X group is retained and only one equivalent of the terminal organometallic RM is required to generate the *lower order*
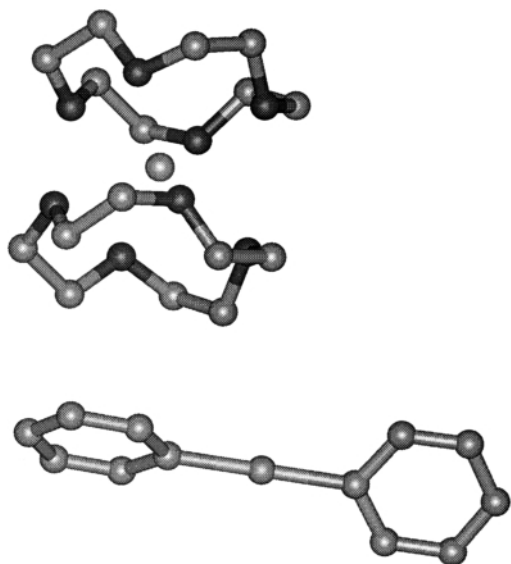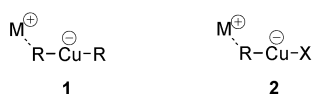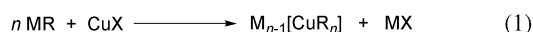
Fig. 1 Crystal structure of the lower order homocuprate [Li(12-crown-4)$_2$][CuPh$_2$]. Hydrogen atoms are omitted for clarity; Cu–C$_\alpha$ 1.925(10) Å, C$_\alpha$–Cu–C$_\alpha$ 178.5°.

cuprate motif **2** [eqn. (2) in Scheme 2]. In this case as the copper is attached to two separate functionalities the product is frequently referred to as a *heterocuprate*. However, the key structural features of **2** are very reminiscent of their *homo-*
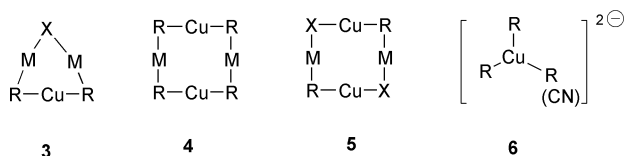
$$n\,MR + CuX \longrightarrow M_{n-1}[CuR_n] + MX \qquad (1)$$

$$MR + CuX \longrightarrow M[Cu(R)(X)] \qquad (2)$$

$$\overset{M^{\oplus}}{\underset{R-Cu-R}{\cdots}}\overset{\ominus}{} \qquad \overset{M^{\oplus}}{\underset{R-Cu-X}{\cdots}}\overset{\ominus}{}$$

$$\mathbf{1} \qquad\qquad \mathbf{2}$$

Scheme 2 Preparation of *homocuprates* **1** and *heterocuprates* **2**.

cuprate analogues **1** (Scheme 2). The group of van Koten have made extensive studies of thiolate derived *heterocuprate* structures and have linked their solution reactivity to their solid state structures *via* EXAFS spectroscopy.[7]

Aside from crystallographic studies, NMR techniques are effective tools for allowing identification of the fragments **1** and **2** in the *solution* structure of cuprates. For example, employing doubly labelled $^{13}CH_3{}^6Li$ for preparation of [LiCuMe$_2$] allows complete extraction of all the scalar ^nJ ($n = 1$–3) C–C and C–H couplings. Modelling this information directly yields the number of Cu–C bonds present in the cuprate.[8] In the case of *lower order cyanocuprates* (**2**, X = CN) similar analyses may be carried out using $^{13}CN^-$.

The counter cations M$^+$ produced in the formation of *lower order cuprates* are potent Lewis acids and this can lead to two effects: (i) sequestration of any MX present in the reaction mixture into the cuprate and (ii) aggregation of the [CuR$_2$]$^-$ fragments. As the majority of cuprate reagents [CuR$_2$]$^-$ **1** are prepared from halide containing CuX (especially X = Br, I) the presence of X$^-$ is often unavoidable (Scheme 2). Under these conditions theoretical calculations[9] suggest that one of the most stable species is **3**. Formation of **3** is supported by colligative

$$\underset{\mathbf{3}}{\overset{\displaystyle X}{\underset{\displaystyle R-Cu-R}{M\quad M}}} \qquad \underset{\mathbf{4}}{\overset{\displaystyle R-Cu-R}{\underset{\displaystyle R-Cu-R}{M\quad M}}} \qquad \underset{\mathbf{5}}{\overset{\displaystyle X-Cu-R}{\underset{\displaystyle R-Cu-X}{M\quad M}}} \qquad \underset{\mathbf{6}}{\left[\overset{\displaystyle R}{\underset{(CN)}{R-\overset{Cu}{}-R}}\right]^{2\ominus}}$$

properties measurements (cryoscopy) on LiCuMe$_2$ generated in the presence of LiI in THF. The derived molecular mass is

consistent with structure **3** X = I.[10] The fact that **3** is often the ground state solution structure of Gilman's reagent in the presence of LiX is not made clear in many papers, especially in the older literature. Co-ordination of LiX into the cuprate structure can supposedly be avoided by working in Et$_2$O, or less practically in Me$_2$S, rather than THF. 'Salt free' cuprates can also be fashioned by direct reaction of LiR with organocopper reagents CuR [*cf.* eqn (2)]. The latter compounds are normally prepared by reaction of LiR with CuX followed by purification to remove LiX. These purifications are frequently hindered by the reactive nature of simple organocopper species; for example, MeCu itself is explosive above ~ 0 °C. Cuprates prepared using these techniques frequently exist as the dimers **4** (or **5** for *heterocuprates*). Explicit proof of such dimeric structures is by no means easy. Cryoscopic molecular mass determination, developed by van Koten and others, has proved the most useful solution technique (Table 1).[10] One or two solid state structures have also been reported of which [LiCuPh$_2$(OEt$_2$)]$_2$ is the most informative (Fig. 2).[6]
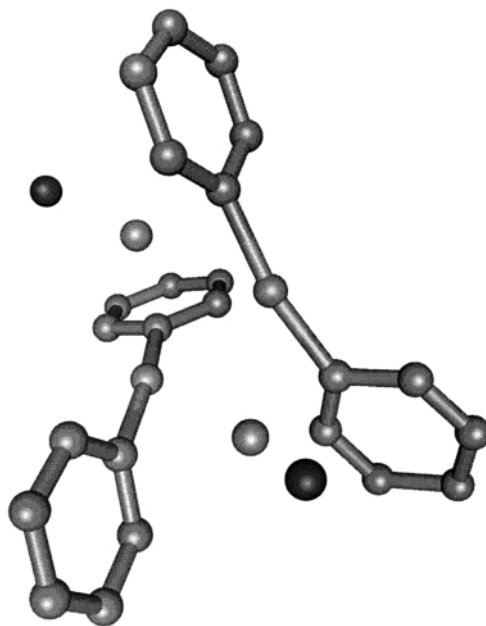

Fig. 2 Crystal structure of the Gilman reagent [LiCuPh$_2$]$_2$ as an etherate solvate. All hydrogens are omitted and only the O-atom of the lithium co-ordinated OEt$_2$ group is shown for clarity. Cu–C$_\alpha$ 1.918(7) Å, C$_\alpha$–Cu–C$_\alpha$ 167.9(3)°.

Does the aggregation state of the ground state cuprate affect the mechanism of 1,4-cuprate? It could be argued, perhaps somewhat contentiously, that for many *lower order cuprates* the answer to this question is no. (For arguments against this proposal see reference 11.) Theoretical studies[12–13] indicate that factors affecting the structure of the *transition state* are much more important. Theoretical modelling also indicates that for aggregated structures **4–5** (M = Li) the lithium atoms carry significant positive charge such that the structures may be almost considered as contact ion pairs. Breakdown of such 'ion pairs' can be effected by only minor changes, for example, the steric difference between [LiCuBu^t(CN)] *vs.* [LiCuPh(CN)]$_2$ (Table 1) or by solvent change from Et$_2$O to THF. Additionally, it is known that the Li$^+$ cations within the *Gilman* dimer **4** undergo rapid exchange with other Li sources if present in the reaction mixture (specifically MeLi) indicating the lability of the cuprate units.[8] While in many instances the dimer **4** may be regarded as a ready source of two [CuR$_2$]$^-$ **1** fragments, *via* dissociation, the combination 'LiCuMe$_2$ + LiI' in diethyl ether should be treated with caution. This particular source of the *Gilman* reagent is the most popular one for mechanistic studies. Although characterised in THF as **3** its exact structure in Et$_2$O

is *unknown*. It is popularly assumed in the literature that it exists as the *Gilman* dimer and that it is not associated with LiI [*e.g.* eqn (1); $n = 2$, MR = LiMe, X = I], but there is little definitive data either to support or refute this suggestion. The reactivity of the LiCuMe$_2$ reagent in Et$_2$O is known to show a dependence on the presence of halide sources. Until definitive information is available on the speciation of 'LiCuMe$_2$ + LiI' in Et$_2$O care must be taken in comparing reactions carried out using this reagent under non-identical conditions. (At present, equilibria involving **4** + LiI associations cannot be ruled out.)

2.2   Are higher order cuprates real?

If *three* equivalents of MR are added to a CuX precursor the stoichiometry of eqn. (1) predicts the formation of a species M$_2$[CuR$_3$]. Based on comparisons with the known cyanide structure, [Cu(CN)$_3$]$^{2-}$ (Cu–C ~ 1.93 Å),[14] such species have been suggested to be able to attain the *higher order cuprate* structure **6** containing three organo functions. The actual structure of cuprates having nominal formulations of [CuR$_3$]$^{2-}$ is a contentious area of cuprate research. Solid state characterisation of an isolated [CuR$_3$]$^{2-}$ unit (R = alkyl, vinyl, or aryl) has not yet been obtained. However, the fragment is found in the larger aggregates of which [Li$_3$(CuPh$_3$)(CuPh$_2$)(SMe$_2$)$_4$] **7**, prepared from CuBr and 3PhLi in SMe$_2$, is a nice example (Fig. 3).[6] The structure of **7** can be analysed as consisting of *higher order* (HO) and *lower order* (LO) parts. In the HO [CuPh$_3$]$^{2-}$ unit the Cu–C$_\alpha$ bonds are significantly longer than in the LO fragment, indicating an electron rich copper species with rather weak Cu–C$_\alpha$ interactions.

The solution structure of **7** is solvent dependent. In dimethyl sulfide ^{13}C NMR studies provide evidence for the presence of a discrete aggregate of formula Li$_2$CuPh$_3$.[15] However, this behaviour is probably due to the special properties of the Me$_2$S as a cuprate solvent (low temperature LiBr precipitation and weaker Li$\cdots$SMe$_2$ interactions strongly favouring aggregation). In *ethereal* solvents there is currently no evidence to support the higher order structures [CuR$_3$]$^{2-}$ **6**. For example, attempted preparation of **7** in THF leads only to *lower order* species. Similarly, reaction of Li^{13}CH$_3$ with THF solutions of [LiCu(^{13}CH$_3$)]$_2$ does not lead to the *higher order cuprate* Li$_2$[Cu(^{13}CH$_3$)$_3$]. Full analysis of the scalar CC and CH coupling constants indicate that essentially no reaction takes place.[8]

In 1981 Lipshutz suggested that an alternative method of attaining a *higher order cuprate* motif would be the addition of *two* equivalents of an organolithium reagent LiR to CuCN. If the strong Cu–CN bond was retained in the product this would fashion the '*higher order cyanocuprate*' species Li$_2$[CuR$_2$(CN)] containing a structural unit analogous to that in **6**.[16,17] Unfortunately, this does *not* happen and attaining the true picture has taken some time (~ 20 years!). At a practical level

Table 1 Selected cuprate aggregation states (in THF) based on colligative property measurement[10]

Cuprate	n^a	Structural type based on ...
[LiCuMe$_2$]$_n$ 'salt free'	~ 2^b	**4**
[LiCuMe$_2$ + LiI]$_n$	~ 1^c	**3**
[LiCuBu^t(CN)]$_n$	~ 1	**2**
[LiCuPh(CN)]$_n$	~ 2	**5**
[Li$_2$CuMe$_2$(CN)]$_n$	~ 1	**3**
[LiCuPh$_2$(CN)]$_n$	~ 1	**3**

^{a} In these experimentally demanding studies the derived value of n normally encompasses a range (typically $n \pm 0.05$ to 0.20). ^{b} Also a dimer in Et$_2$O. ^{c} A dimer (n ~ 2) is indicated in Et$_2$O in the presence or absence of LiI but no information about the speciation of the LiI (if present) is gathered by such experiments.
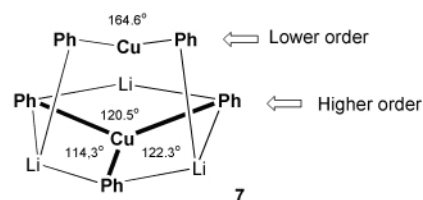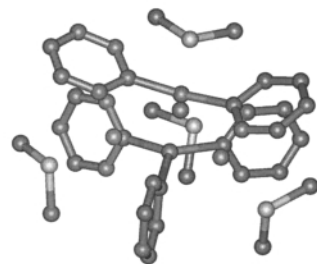
All Li atoms have one or two SMe$_2$ units co-ordinated.

Fig. 3 Structure of [Li$_3$(CuPh$_3$)(CuPh$_2$)(SMe$_2$)$_4$] **7** and its analysis as *higher order* (HO) and *lower order* (LO) *cuprate* fragments. Cu–C$_\alpha$(HO) 2.039(4), 2.000(4), 2.032(4) Å. Cu–C$_\alpha$(LO) 1.916(5), 1.942(4) Å.

the cuprate recipe '2LiR + CuCN' can sometimes lead to reagents of improved reactivity compared to classical *Gilman* cuprates LiCuR$_2$ and extensive investigations by Lipshutz centred on this reactivity difference.[17] Only recently, however, has appropriate structural, NMR and theoretical data become available on these species.[16] Theoretical studies suggest that the ground state structure of '*higher order cyanocuprates*' is in fact a *lower order* structure containing sequestered LiCN, as in **3** (M = Li, X = CN).[16] In support of this proposal no $^2J_{CC}$ NMR couplings can be detected between the R and CN functions in these species (they are present in compounds **2**, X = CN). Solution X-ray studies (EXAFS) also discount the presence of any strong Cu–CN contact. Representative '*higher order cyanocuprates*' are monomeric by cryoscopy, consistent with structure **3**. As CN$^-$ is not spherical the question arises as to how it is bound between the two lithium cations of structure **3**. By comparing the experimentally observed ^{15}N NMR chemical shifts of *cyanocuprates* containing [C^{15}N]$^-$ with those calculated theoretically Snyder and Bertz have suggested that the species [Li$_2$CuBu$_2$(CN)] binds the cyanide unit as Li(μ-CN)Li with both Li$\cdots$C and Li$\cdots$N contacts.[18] The presence of this unit has been found in the first two crystal structures of '*higher order cyanocuprates*' but in these cases the presence of chelating amine functions result in solvent separated rather than contact ion pairs, as determined by Boche.[16] As the structure **3** is firmly established the term '*higher order cyanocuprate*' is inappropriate and an alternative name, *cyano-Gilman cuprates,* has been suggested.[18]

3   The mechanisms for cuprate addition—π-complexes, yes, but copper(III)?

The definition of a reaction mechanism requires the model to exactly predict the kinetic behaviour of the evolving reaction. Only two kinetic studies are available in the area of 1,4-cuprate additions to enones thus far. The currently accepted mechanism, based on these studies, is shown in Scheme 3 (for early ideas involving electron transfer see references 2 and 11).

In the most cited work in this area, Krauss and Smith[19] determined values of K and k_1 by stopped flow techniques in a kinetic regime consistent with Scheme 3. An initial equilibrium mixture contained an intermediate that underwent decay to enolate **10** without detection of any subsequent rest state. The initial intermediate was assumed to be a π-complex **9**. Under the conditions of this early study (25 °C, Et$_2$O) many cuprates and
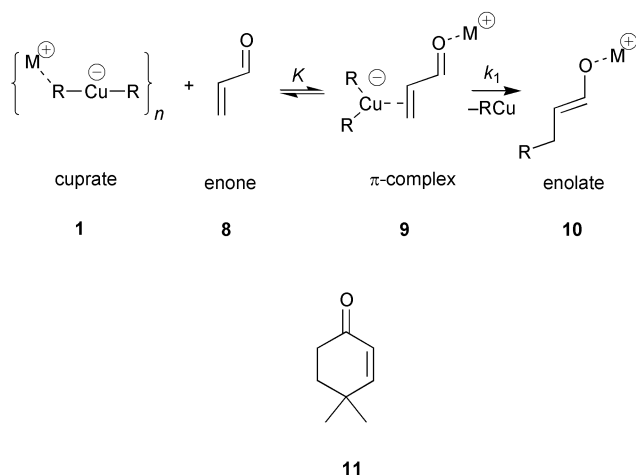
Scheme 3 Mechanism for 1,4-cuprate addition to enones (represented by a generic acrolein structure), M is normally lithium.

enolates are unstable. Additionally, to slow the reaction down sterically encumbered enones were used and in some cases complete clean conversion to the enolate product was not observed. Whether these factors have had any effect on the data obtained is not clear. In a recent study Krause and co-workers have obtained rate data for the transformation of **9** to **10** using enone **11** and LiCuMe$_2$·LiI.[20] These data support a first order transformation with k_1 values between 0.0011 s^{-1} (-69 °C) and 0.012 s^{-1} (-58 °C). In the absence of significant primary kinetic data, mapping of the reaction co-ordinate has involved a combination of NMR studies and the interception of reactive intermediates ('trapping') supported by theoretical studies. These data are considered in the following sections.

3.1 Cuprate enones interaction—carbonyl binding and C=C π-complexation

In an enone, two potential binding sites exist: the lone pairs on the carbonyl oxygen and π-electron cloud of the double bond.

The former seeks out 'hard' oxophilic, often charged, Lewis acids (Li$^+$, MgX$^+$, *etc.*) with free co-ordination sites.[21] The presence of such strong Lewis acids associated with the cuprate is essential for 1,4-addition. For example, Li(12-crown-4)$_2$CuPh$_2$, co-ordinatively saturated at Li$^+$ (Fig. 1), does not react with enones. Conversely, the 'soft' [CuR$_2$]$^-$ cuprate co-ordinates the π-bond. Theoretical calculations suggest bending of the [R–Cu–R]$^-$ fragment to an angle of *ca.* 150° and re-hybridisation at both copper and the 'ene' fragment consistent with Chatt–Dewer d-π* back donation model.[22] Overall, the enone binding may be considered the product of successive equilibria (Scheme 4).

NMR spectroscopy has proved a powerful method for the detection and characterisation of the π-complexes **9**. On co-ordination of the O(1) carbonyl oxygen by Li$^+$ the ^{13}C NMR shift of the carbonyl carbon C(2) typically suffers a small shift to higher frequency (downfield) of +1 to +10 ppm while formation of a π-complex results in a large shift to lower frequency (upfield) of -40 to -80 ppm for the alkene carbons C(3) and C(4). For example, the mixture **14** is generated by LiCuMe$_2$·LiI addition to (E)-methylcinamate.[11] Use of a high cinamate:cuprate ratio favoured formation of the lithium complex **14LA** while using an excess of low halide content LiCuMe$_2$ favoured the π-complex **14π**.

In a closely related study the mixture **15** was prepared similarly and dynamic exchange between **15LA** and **15π** established.[23] The identity of **15LA** was established by comparison with the ^{13}C NMR shifts of the parent enone in the presence of LiI or LiClO$_4$ alone and by noting that this component of the equilibrium mixture shows no upfield shift for the alkene signals C(3) and C(4). The data obtained in these experiments do not allow differentiation between the "open" structures shown in **14** and **15** and equivalent "cyclic" structures having Cu–R–Li–O(1) intramolecular contacts. Krause prefers the latter 'cyclic' motif and examples **16**–**17** are taken from his work.[24] Brilliant red–orange **16** is formed from the parent enynoate and Li$_2$[Cu(Bu^t)$_2$CN] at -80 °C. By using ^{13}C labelled materials the $^1J_{C(3),C(4)}$ coupling constants for this species can be obtained. The value obtained for the π-complex
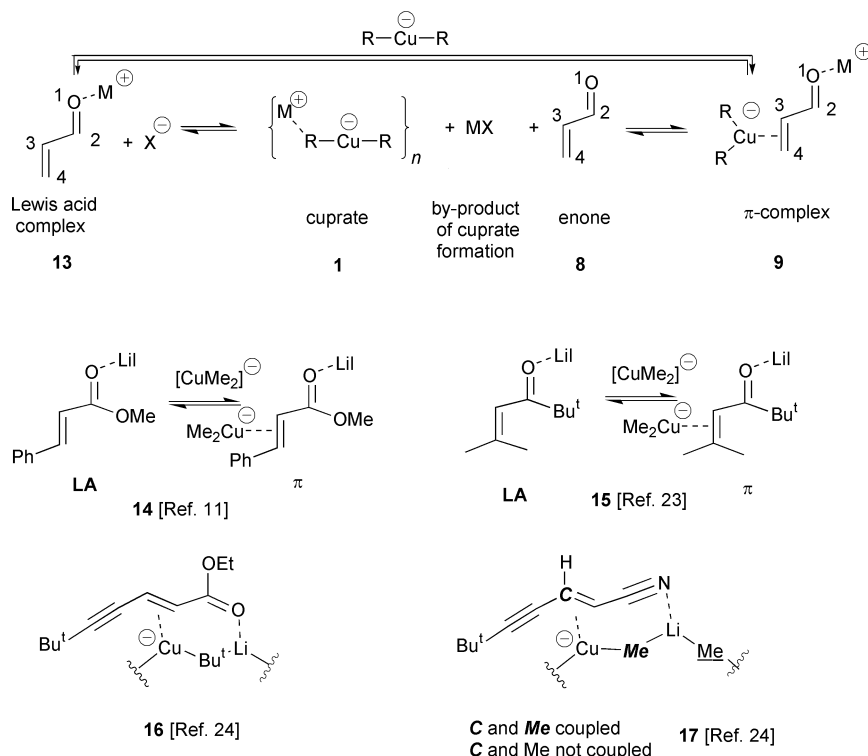
Scheme 4 Equilibrium formation of Lewis acid and π-complexes from cuprates and enones (represented by a generic acrolein structure) and specific characterised examples.

is around 20 Hz, lower than in the parent α,β-unsaturated ester indicating a reduction in the bond order consistent with re-hybridisation of the sp^2 double bond to a higher sp^3 contribution. In samples of **16** a second set of signals is apparent. This is not due to the formation of a Lewis acid complex as in **14**–**15** as an upfield shift for C(3) and C(4) is apparent in both signal sets. A mixture of two different aggregation states is proposed to account for this observation. The ^{13}C labelled π-complex **17** demonstrates J_{CC} coupling of 12 Hz to only one of the inequivalent methyl groups present in the cuprate. This result strongly suggests that only one of the two Cu–Me functions is in close proximity to the double bond of the enone. Based on this coupling constant value the strength of the Cu–alkene π bond in **17** is about half that in Li[CuMe(CN)].

3.2 Copper(III) *vs.* carbocupration

As no additional species have been detected in the transformation of the π-complex **9** to enolate **10** only indirect methods can be used to characterise the key C–C bond forming step. Two principal mechanistic possibilities exit. One possibility is formation of a d^8 copper(III) peralkyl intermediate **18** by formal oxidative addition followed by reductive elimination to the CuR adduct **20** (Scheme 5). Alternatively, **9** could undergo 1,2-migratory insertion fashioning the new cuprate **19**, which on rearrangement leads to the same CuR adduct **20**.

At this point it is appropriate to say something about the fragment Cu(Alkyl)$_3$ in intermediate **18** to which a formal Cu(+3) oxidation state has been assigned. All recent theoretical calculations in this area indicate that it is *the organic ligands* that undergo significant oxidation (to Alkyl$^{\delta+}$) and reduction (to Alkyl$^{\delta-}$) in the formal oxidative addition–reductive elimination cycle while the metal remains close to Cu^I. However, for the present, **18** will be represented as a formal Cu^{III} intermediate but we will return to this Cu^{III}(Alkyl)$_3$ *vs.* Cu^I(R)(R$^+$)(R$^-$) theme later.

Recent developments in Density Function Theorem (DFT) may offer the possibility to distinguish between **18** and **19** in both model and real systems. Most calculations have concentrated on reaction co-ordinates approaching **18**, the work of both Snyder and Nakamura being foremost in this area. Theoretical interaction (DFT) of acrolein with the Gilman dimer [LiCuMe$_2$]$_2$ leads rapidly to the formation of the π-complex **21** (Fig. 4) which differs from **9** only in the presence of an extra LiCuMe$_2$ unit.^{12} The calculations predict that some of the
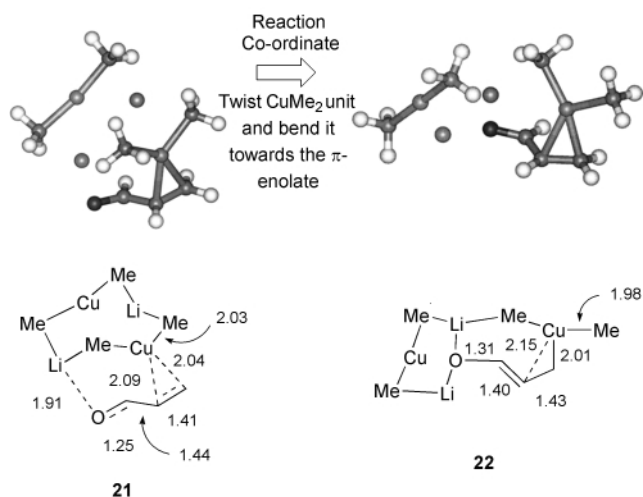
Fig. 4 Alternative π-complex **21** and Cu^{III} allyl **22** precursors to the key C–C bond forming step in [LiCuMe$_2$]$_2$ addition to acrolein. Bond distances in Å.

properties of **21** are in accord with the spectroscopically observed **14**–**17**.

Thus, an elongated C(3)–C(4) bond is observed consistent with the ^{13}C J_{CC} coupling data of Krause. The four Cu–C distances in **21** range 2.025–2.089 Å while the charge analysis shows significant electron transfer from the copper to the acrolein oxygen (>0.8 e$^-$). Rearrangement of the π-complex **21** leads to a somewhat energetically more stable species **22**. The Cu–C(4) distance shortens while the copper moves slightly backwards towards the centre of the developing C(2)=C(3) enolate double bond [the Cu–C(2) distance falls from 2.62 to 2.43 Å on conversion of **21** into **22**]. Formally this species may be thought of as a Cu^{III} allyl species with π-donation from the enolate double bond. However, natural charge analysis of the copper indicates only a rise of *ca.* +0.8 at the metal. In some instances **22** may be a better model of the pre-transition rest state **9** than **21**. Consistent with this picture, ^{13}C NMR chemical shift data calculated on structures of type **22** reproduce those observed experimentally for **15** and related species.^{13} Further theoretical development of the reaction co-ordinate from **22** leads first to transition state **23** which fashions a MeCu adduct analogous to **20** (Fig. 5). The geometry of this transition state has also been found in calculations on [LiCuMe$_2$]$_2$ additions to both cyclohex-2-enone and acetylene.^{12} The question arises as to how the formal copper(III) intermediate in transition state **23**
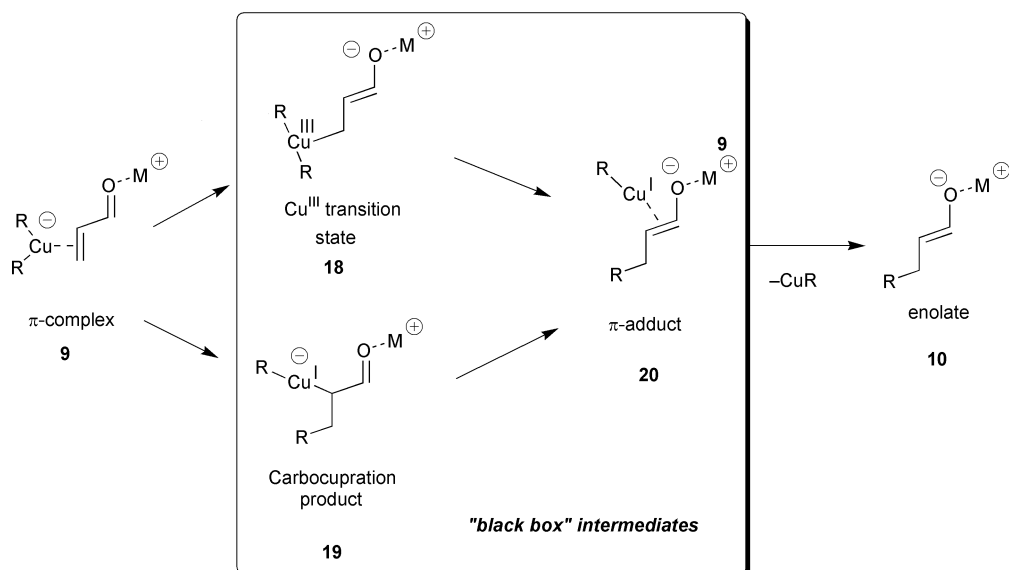
Scheme 5 Oxidative addition *vs.* carbocupration possibilities for the C–C bond forming step in 1,4-cuprate addition to a generic acrolein.
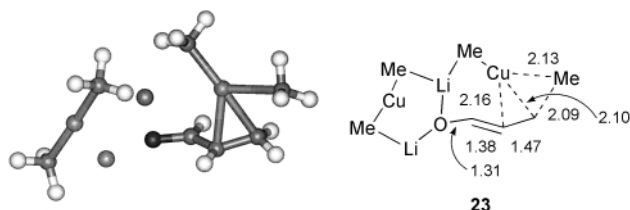
Fig. 5 Transition state **23** for C–C bond formation in [LiCuMe$_2$]$_2$ addition to acrolein. Bond distances in Å.

is stabilised? Most levels of theory indicate that T-shaped CuR$_3$ are rather high-energy species that exist in only shallow energy minima. However, calculations suggest that interaction of the CuR$_3$ unit with σ-donor ligands results in the formation of CuR$_3$(S) (S = solvent or ligand) of significantly increased stability.[25] In transition state **23** donation from the enolate plays a similar role. It is likely that the large rate accelerations observed in CuR(PR$_3$)$_n$-catalysed ZnEt$_2$-to-enone additions[4] have their origin in similar affects attributable to strong P→Cu donation. Charge analyses of CuR$_3$(S) species indicate an ionic bonding scheme with the oxidation state for copper only a little greater than +1. Certainly these species only formally contain a Cu^{III} centre with three covalently bound organo functions. An extreme example of the degree of stabilisation that this regime can afford is shown by the isolation of [Cu(CF$_3$)$_4$]$^-$.[26] The bonding in this species can be analysed as '[Cu(CF$_3$)$_2$ + CF$_3^-$ + CF$_3^+$]$^-$'. It has been suggested that equivalent behaviour accounts for the increased stability of Cu^{III}R$_2$(CH$_2$CH=CHO-Li)(S) transition states in conjugate addition. In a simple way these can be thought of as Cu^{I}R$_2$($^-$CH$_2$CH=CHOLi)(S$^+$) entities.[25]

By extracting the enone fragment, along with the developing C–C bond, from transition states related to **23** some progress can be made in correlating the molecular mechanics of 3-substituted cyclohexenones to the observed stereochemistry in the ketone product.[13] For **24** (R = Me; Scheme 6) axial attack
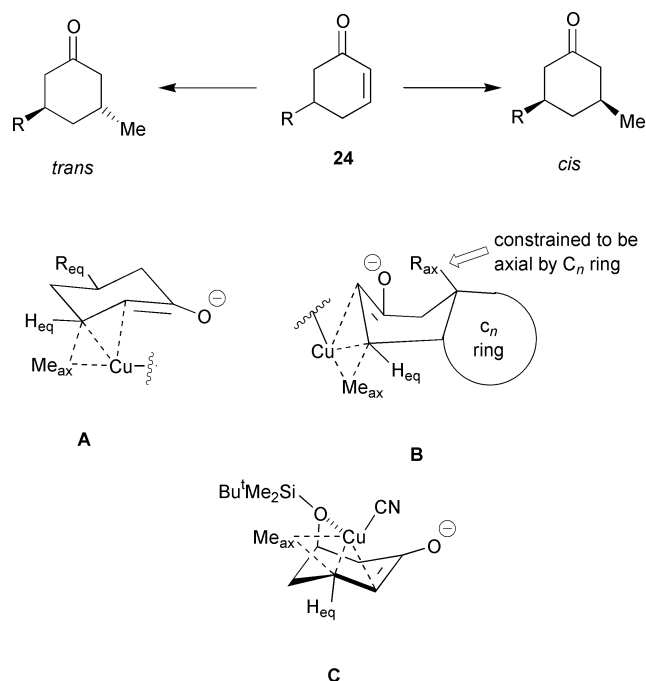

Scheme 6 Transition states for cuprate additions to 3-substituted cyclohexenones. In transition states **A** and **B** only part of the cuprate is shown for clarity.

of the cuprate (transition sate **A**) constitutes a lower energy pathway than for the equivalent equatorial face approach.

The calculations rationalise the observed *trans* stereochemistry seen in these reactions.[13] If the 3-substituent is constrained

to adopt an axial position from being part of a bicyclic ring system then calculations indicate that the boat transition state **B** is energetically favoured. Finally, substituents capable of co-ordinating *lower order cyanocuprates* lead to high levels of *cis* stereoselectivity, *e.g.* **24** (R = OSiBu^{t}Me$_2$).[27] Theoretical studies have not yet been applied to this latter system but the observed stereochemical outcome can be rationalised by the intramolecular co-ordination in transition state **C**.

Although recent theoretical calculations have concentrated on the mechanisms that at least formally operate *via* a copper(III) intermediate there is one strong piece of evidence to support the alternative carbocupration mechanism (*via* **19**, Scheme 5).[28] Use of an appropriate tin precursor allows the formulation of the homocuprate **25** at −78 °C (Scheme 7). This unusual cuprate
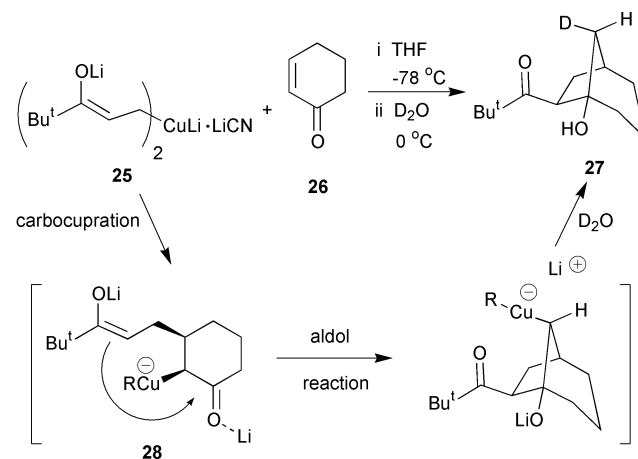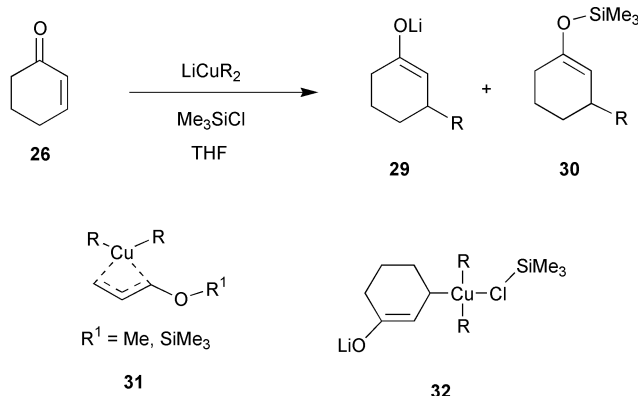

Scheme 7 Evidence for carbocupration in conjugate addition chemistry.

contains a 'built in' enolate. When **25** is treated with cyclohexenone **26** and the reaction quenched at 0 °C with D$_2$O the major product isolated is the labelled bicyclic alcohol **27**. The formation of **27** as a single stereoisomer is *not* easily explained by a mechanism involving a formal copper(III) route (*cf.* **18**, Scheme 5). Simple *syn* addition of the Cu–C$_\alpha$ bond forming **28** followed by ring closure is, however, consistent with the observed product.

The comparable viability of routes *via* a formal Cu^{III} transition state **18** and a carbocupration intermediate **19** have been investigated by studying the ^{13}C kinetic isotope effects (KIEs) in the reaction of LiCuBu$_2$ (prepared from BuLi and CuBr·SMe$_2$) and cyclohexenone **26**.[29] The results are claimed to be more in accord with the reaction profile shown in Figs. 4–5. However, the exclusion of a carbocupration mechanism was based on comparison of the experimental data to those KIEs calculated for [CuMe$_2$]$^-$ addition to ethene. How good a model such is for systems like **26** is not clear at present.

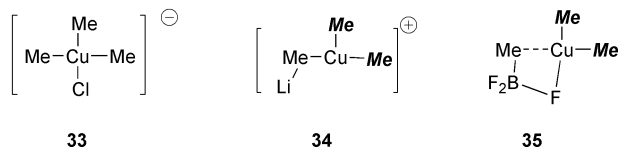### 3.3 The effect of the additives Me$_3$SiCl and BF$_3$ on 1,4-cuprate additions

Empirically it is found that addition of Me$_3$SiCl (TMSCl) or BF$_3$·OEt$_2$ to cuprate–enone mixtures frequently results in a dramatic increase in the rates of such reactions. The effect of TMSCl addition has recently been reinvestigated by Bertz and co-workers who find that only reactions carried out in THF are accelerated.[30] In these reactions TMS enol ethers are frequently isolated. For example, reaction of LiCuR$_2$ with cyclohexenone **26** and TMSCl in THF affords only traces of the 3-alkylcyclo-hexanone **29** and principally the enol ether **30** (Scheme 8). The question arises: does the Si–O(1) bond form during the conjugate addition transition state (as originally suggested by Corey) or subsequently through silylation of an initially formed enolate (as initially suggested by Bertz)? The ratio of **29**:**30** in

Scheme 8 Rate acceleration of cuprate addition by TMSCl.

structure **16**. No further intermediates can be detected, but if this were followed by oxidative addition the formal Cu^{III} intermediate **40** would result. Direct reductive elimination of **40** would fashion the simple conjugate addition product. However, the lifetime of **40** must be sufficient to allow rearrangement to non-observed allenic copper(III) intermediate **41** before loss of CuR leading to the observed 1,6-addition product enolate (Scheme 9). This kind of behaviour appears to be viable for up to 1,12-cuprate additions.[32]

the initial stages of the reaction should answer this question but such experiments are complicated by the ready hydrolysis of **30**. The best current data favour the Corey proposition. Two theoretical proposals have been put forward as the origin of the TMS rate acceleration. Alkylation of the π-complex **9** leads to a defined new species **31** (R^1 = Me)[25] which is closely related to the original Corey 'd,π*' silylated intermediate **31** (R^1 = SiMe$_3$) which collapses to the enol ether **30**. Alternatively, it has been suggested that formation of the 'Cu(III)' σ-adduct **32** lowers the barrier to reductive elimination by an organometallic analogue of the Eaborn effect (carbocation stabilisation by β-silicon).[30] It has been suggested that the absence of a TMSCl acceleration effect in the reaction of cuprates with enones in *diethyl ether* is indicative of a reaction co-ordinate featuring interaction of the dimer [LiCuR$_2$]$_2$ with the enone (*e.g.* Figs. 4–5).[30] Conversely, the presence of a TMSCl effect in THF has been taken to indicate the presence of either exclusively monomeric **9** or a greatly reduced contribution from the dimeric forms **21**–**23**.[30]

Calculations on the interaction of CuMe$_3$ (as a model of transition state **18**) with Cl$^-$, Li$^+$, and BF$_3$ provide a good rationale for the rate acceleration phenomenon exhibited by BF$_3$ in cuprate additions.[31] The species [CuMe$_3$Cl]$^-$ **33** is con-
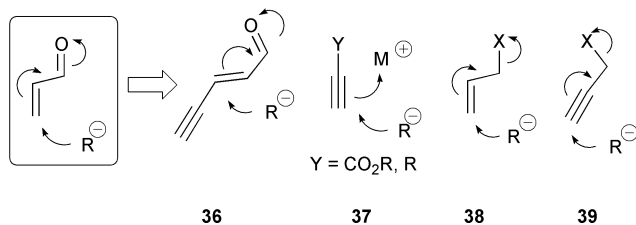

siderably stabilised compared to T-shaped CuMe$_3$, which is kinetically unstable. However, the barrier to reductive elimination in **33** is very high (18.0 kcal mol^{-1}). Conversely, co-ordination of a lithium to one of the methyl groups in [LiMeCu*Me*$_2$]$^+$ **34** leads to spontaneous reductive elimination of *Me–Me*. The CuMe$_3$·BF$_3$ adduct enjoys both these effects. Although the formal Cu^{III} centre is stabilised the intermediate formed, **35**, is still kinetically labile. The barrier to reductive elimination of ethane is only 4.3 kcal mol^{-1}, thus explaining the rate acceleration observed through addition of BF$_3$.
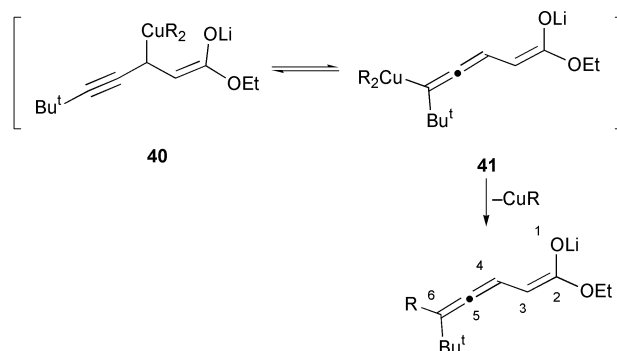
4   Reactions mechanistically related to 1,4-cuprate addition

Cuprate addition to extended Michael acceptors,[32] such as **36**, additions to ynones or alkynes **37**, and S$_N$2′ displacements from allylic **38** or propagylic **39** halides all involve the formation of one C–C bond and formal transfer of two electrons to an appropriate acceptor in the substrate. Formally these reactions are analogous to 1,4-cuprate addition to enones.

The initial reaction co-ordinate in the addition of cuprates to enynes type **36** involves π-complex formation, for example


Scheme 9 Equilibrating copper(III) species in formal 1,6-cuprate additions to enynes.

Alkyne carbocupration **37** is closely related to one of the proposed mechanistic pathways for 1,4-cuprate addition to enones. However, in contrast to the proposed transient **19**, under favourable conditions the σ-alkenyl intermediates may be spectroscopically observed. For example, in the reaction of Bu^{t}C≡CCO$_2$Me with THF solutions of LiCuMe$_2$·LiI Krause observed formation of *cis*-**42** (R = Me; X = I). The equivalent
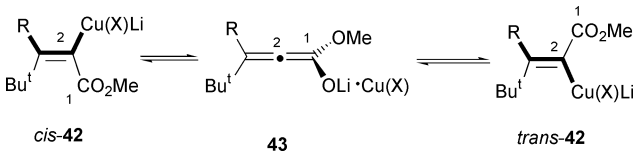
Scheme 10 Spectroscopically observed intermediates resulting from cuprate additions to ynones.

reaction when carried out in diethyl ether leads to a *cis–trans* mixture implying the presence of equilibria involving the allenoate **43** (Scheme 10). Compound **43** can be trapped as its TMS-ether by addition of Me$_3$SiCl. Alternatively, reaction of Bu^{t}C≡CCO$_2$Me with LiCuBu^t$_2$·LiCN leads directly to **43** (R = Bu^t; X = CN) based on the measured 1,2-CC ^{13}C NMR coupling constant of 137 Hz.[33]

The closely related additions of [CuMe$_2$]$^-$, LiCuMe$_2$, and the aggregate LiCuMe$_2$·LiI (**3**; M = Li, X = I) to acetylene have been studied theoretically.[12] The presence of the lithium is crucial in lowering the activation barrier to those observed in the synthetic transformation (~ 16 kcal mol^{-1}). Interestingly, the lowest energy species does not involve a carbocupration mechanism but the formation of a 'Cu^{III}' intermediate in the interaction of **3** with acetylene. The transition state (Fig. 6) is reached by significant electron transfer from copper resulting in a transient Cu–C bond while the developing vinylic carbanion is trapped by a lithium cation. Subsequent intramolecular transmetallation affords carbocuprated species analogous to those
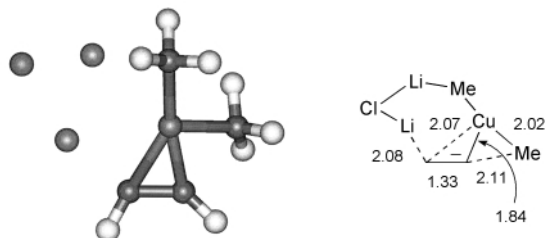
Fig. 6 Calculated transition state for addition of **3** (M = Li, X = Cl) to acetylene. Bond distances in Å.

observed by Krause above. Based on these theoretical studies it has been proposed that direct carbocupration *vs.* oxidative addition (*cf.* Fig. 5) can account for the differing regiochemistries that are sometimes observed for intermediates trapped in the S_N2' reactions of propargylic halides with organocuprates (structure **39**).[12] Despite its rather simplistic relationship to 1,4-cuprate addition S_N2' substitution chemistry (structures **38**–**39**) offers a wide range of mechanistic possibilities. These are mainly due to the diverse range of Lewis acid-leaving group interactions possible in the reaction co-ordinate. The suggestion that many leaving group transition states are accessible for such substrates is supported by the difficulties that synthetic chemists have had in developing enantioselective copper-based catalysts for this reaction.[34]

5   Conclusions and outlook

In the last few years very significant inroads have been made into understanding of the intimate routes by which organocuprate species carry out their remarkable transformations. In particular, theoretical studies have recently entered a regime whereby they are able to suggest mechanistic experiments to synthetic chemists with an increasing degree of reliability. The prediction of the existence of structure **3** before the first physical evidence appeared to support this formulation is a notable example. At present, such approaches are the only way to interrogate the structure of the oxidative addition products $[R_2Cu(CH_2CH=CHOM)]^-$ (*cf.* Fig. 5). However, the theoretical predictions that suitable donor ligands can stabilise such species may yet lead to the observation of such transients as $[R_2Cu(CH_2CH=CHOM)^-(S^+)]^-$ with suitably strong donors (S). Formally these species are copper(III), but the natural population analyses (NPA) that these intermediates show cause us to modify our views of formal oxidative addition. It is just that—a formalism; NPA of the intermediates in 1,4-cuprate indicate that the electronic action is very much ligand centred. In one sense Cu[III] species in the cuprate reaction co-ordinate have already been observed. Calculations on the π-complexes that are frequently studied by NMR indicate that these are at least as oxidised as the hypothetical Cu[III] transition state.

Exciting possibilities exist for the interaction of theoreticians and experimentalists in the near future. For example, the evidence for a carbocuparation mechanism obtained by Ryu[28] clearly requires theoretical investigation and further attempts to trap the σ-copper intermediate. Recently developed NMR techniques allowing rapid low temperature mixing of reactive enones and cuprates may afford ways to study this and related systems.[35] Similarly, the recent calculations on BF$_3$ interaction with $[CuMe_3]^-$ clearly have implications for general Lewis acid cuprate activation especially in the field of asymmetric catalysis.

6   Acknowledgements

7   References

1 Review—overview and checked recipes for organocuprate synthesis: *Organocopper Reagents—A Practical Approach*, ed. R. J. K. Taylor, Practical Approach in Chemistry Series, Series eds. L. M. Harwood and C. J. Moody, Oxford University Press, 1994.
2 Review—cuprate use in synthesis: J. A. Kozlowski, in *Comprehensive Organic Synthesis*, ed. B. M. Trost and I. Fleming, Pergamon, Oxford, 1991, vol. 4, ch. 1.4, pp. 169–198.
3 Review—cuprate synthesis, structure and use: N. Krause, *Angew. Chem., Int. Ed. Engl.*, 1997, **36**, 186.
4 Review—recent enantioselective additions: N. Krause, *Angew. Chem., Int. Ed. Engl.*, 1998, **37**, 283 and references therein.
5 H. Gilman, R. G. Jones and L. A. Woods, *J. Org. Chem.*, 1952, **17**, 1630.
6 Review—crystallographically characterised cuprates: P. P. Power, *Prog. Inorg. Chem.*, 1991, **39**, 75 and references therein.
7 (*a*) Review—arenethiolate derived cuprates: G. van Koten, *Pure Appl. Chem.*, 1994, **66**, 1455; (*b*) J. H. Bitter, B. L. Mojet, M. D. Janssen, D. M. Grove, G. van Koten and D. C. Koningsberger, *J. Synchrotron Rad.*, 1999, **6**, 423.
8 T. Mobley, F. Muller and S. Berger, *J. Am. Chem. Soc.*, 1998, **120**, 1333 and references therein.
9 J. P. Snyder and S. H. Bertz, *J. Org. Chem.*, 1995, **60**, 4312.
10 A. Gerould, J. T. B. H. Jastrzebski, C. M. P. Kronenburg, N. Krause and G. van Koten, *Angew. Chem., Int. Ed. Engl.*, 1997, **36**, 755 and references therein.
11 C. Ullenius and B. Christenson, *Pure Appl. Chem.*, 1988, **60**, 57; G. Hallnemo, T. Olsson and C. Ullenius, *J. Organomet. Chem.*, 1985, **282**, 133.
12 E. Nakamura, S. Mori and K. Morokuma, *J. Am. Chem. Soc.*, 1997, **119**, 4900 and other papers in this series summarised at http://WWW.chem.s.u-tokyo.ac.jp/~common/HTML/3D.structure.htm
13 S. Mori and E. Nakamura, *Chem. Eur. J.*, 1999, **5**, 1534 and references therein.
14 P. Chaudhuri, K. Oder, K. Wieghardt, J. Weiss, J. Reedijk, W. Hinrichs, J. Wood, A. Ozarowski, H. Stratemaier and D. Reinen, *Inorg. Chem.*, 1986, **25**, 2951.
15 S. H. Bertz and G. Dabbagh, *J. Am. Chem Soc.*, 1988, **110**, 3668.
16 Review—higher order cyanocuprates: N. Krause, *Angew. Chem., Int. Ed.*, 1999, **38**, 79 and references therein, especially G. Boche, F. Bosold, M. Marsch and K. Harms, *Angew. Chem, Int. Ed.*, 1998, **37**, 1684.
17 Review—synthetic use of 'higher order cyano cuprates': B. H. Lipshutz, *Synthesis*, 1987, 325.
18 S. H. Bertz, K. Nilsson, O. Davidson and J. P. Snyder, *Angew. Chem., Int. Ed.*, 1998, **37**, 314.
19 S. R. Krauss and S. G. Smith, *J. Am. Chem. Soc.*, 1981, **103**, 141.
20 J. Canisius, A. Gerold and N. Krause, *Angew. Chem., Int. Ed.*, 1999, **38**, 1644.
21 Review—Lewis acid binding of carbonyl groups: S. Shambayati and S. L. Schreiber, in *Comprehensive Organic Synthesis*, ed. B. M. Trost and I. Fleming, Pergamon, Oxford, 1991, vol. 1, ch. 1.10, pp. 283–353.
22 S. Mori and E. Nakamura, *Tetrahedron Lett.*, 1999, **40**, 5319.
23 A. S. Vellekoop and R. A. J. Smith, *J. Am. Chem. Soc.*, 1994, **116**, 2902.
24 N. Krause, R. Wagner and A. Gerold, *J. Am. Chem. Soc.*, 1994, **116**, 381.
25 J. P. Snyder, *J. Am. Chem. Soc.*, 1995, **117**, 11025.
26 J. P. Snyder, *Angew. Chem., Int. Ed. Engl.*, 1995, **34**, 80.
27 G. Hareau-Vittini, S. Hikichi and F. Sato, *Angew. Chem., Int. Ed.*, 1998, **37**, 2099.
28 I. Ryu, H. Nakahira, M. Ikebe, N. Sonoda, S. Yamato and M. Komatsu, *J. Am. Chem. Soc.*, 2000, **122**, 1219.
29 D. E. Frantz, D. A. Singleton and J. P. Snyder, *J. Am. Chem. Soc.*, 1997, **119**, 3383.
30 S. H. Bertz, A. Chopra, M. Eriksson, C. A. Ogle and P. Seagle, *Chem. Eur. J.*, 1999, **5**, 2680 and references therein.
31 E. Nakamura, M. Yamanaka and S. Mori, *J. Am. Chem. Soc.*, 2000, **122**, 1826.
32 Review—additions to extended Michael acceptors: N. Krause and S. Thorand, *Inorg. Chem. Acta*, 1999, **296**, 1.

33 K. Nilsson, T. Andersson, C. Ullenius, A. Gerold and N. Krause, *Chem. Eur. J.*, 1998, **4**, 2051.

34 F. Düber and P. Knochel, *Angew. Chem., Int. Ed.*, 1999, **38**, 379.

35 S. H. Bertz, C. M. Carlin, M. D. Murphy, C. A. Ogle and H. P. Seagle, *Abstracts of Papers of Am. Chem. Soc.*, 215th Meeting, San Francisco, 26–30 March 2000, ORG 646 and 648.